Desalination and Water Treatment
www.deswater.com
doi: 10.1080/19443994.2014.941303

56 (2015) 646–654
October

Taylor & Francis
Taylor & Francis Group

Speciation of iron and development of iron corrosion scales in drinking water distribution systems

Haoqiang Tan[a,b,*], Wenjie He[a,b], Hongda Han[a], Yingchen Lu[a], Nan Zhang[a]

[a]*School of Municipal and Environmental Engineering, Harbin Institute of Technology, Harbin 150090, China, Tel. +8615900285261; email: tanhaoqiang126@126.com (H. Tan), Tel. +8613902008535; email: tianjinwater@sohu.com (W. He), Tel. +8618602673311; email: hanhongda@sina.com (H. Han), Tel. +861375231497; email: lycbaggio@sina.com (Y. Lu), Tel. +8613920743999; email: 36213345@qq.com (N. Zhang)*
[b]*Tianjin Waterworks Group Co., Ltd, Tianjin 300040, China*

Received 2 January 2014; Accepted 26 June 2014

ABSTRACT

The major objective of this work is to study the speciation of iron impacted by water quality including dissolved oxygen (DO), pH, alkalinity, sulfate, chloride, and monochloramine and the development of iron corrosion scales in drinking water distribution systems. Alkalinity, pH, and monochloramine had significant impacts on iron oxidation rate, and suspended iron particle, and DO, sulfate, and chloride had a slight effect on iron oxidation rate and suspended iron particle. Except at low pH, the oxygenation process of ferrous iron to ferric iron can be well described by oxidation kinetics model which also fits the monochloramine oxidation reaction. In the initial experiment stage with pipe corrosion scales having been destroyed and the iron being released seriously, the newly formed free and amorphous iron contents increased, instable iron compound dominated the iron corrosion scales and the mass fraction of the total iron in iron corrosion scales rose. With the iron release amount being relatively stable, the free and amorphous iron contents dropped, magnetite and goethite were the main components of iron corrosion scales, and the total iron in iron corrosion scales decreased.

Keywords: Iron; Oxidation; Kinetics; Suspended iron particle; Corrosion scale

1. Introduction

Discolored water is a large proportion of drinking water consumer complaints, which may be caused by relatively insoluble ferric iron coming from pipe materials, including cast iron, steel, ductile iron, and galvanized and cement-lined iron [1,2]. Numerous research reports [3–9] have been published on effect factors of iron release in drinking water distribution systems (DWDSs), such as sulfate, chloride, dissolved oxygen (DO), pH, alkalinity, residual chlorine, source water blending, hydraulic retention time, flow velocity, and change of flow direction. In addition, discolored drinking water resulting from the properties of iron chemical forms is commonly referred as "red" or "yellow" water, which can stain clothing and fixtures, and contribute to metallic tasting tap water. The properties of iron chemical forms are important in the properties of iron corrosion scales and deposits, iron release mechanisms, the color and turbidity of aqueous iron suspension, and iron particle deposition rate.

*Corresponding author.

However, very little practical information is available on how water quality impacts ferrous iron oxidation rate and the properties of iron particles in DWDSs.

Iron-based metals are common pipe materials used to distribute drinking water from the water treatment plant to the consumer's tap. Corrosion of iron materials is a serious problem in DWDSs, which can negatively impact water quality [2,10–13]. Iron corrosion is mainly described as non-uniform in nature and is typically characterized by localized pitting corrosion and thick tuberculate growth of corrosion deposits and scales, which can lead to significant water flow restrictions and jeopardize structural pipe integrity [2,14–17]. Iron corrosion by-products are iron compounds, which are often layered in structure and a mixture of reduced and oxidized iron phases. However, the chemical characteristics of iron corrosion scales at different iron release stages are seldom studied.

Because the water quality indices including DO, pH, alkalinity, sulfate, chloride, and monochloramine vary in different DWDSs and seasons, and are critical to iron release, the primary objective of this paper is to study their impacts on the ferrous iron oxidation rate and suspended iron particle, and determine ferrous iron oxidation behavior and rate constants. Since iron corrosion and release can cause a shift of one kind of iron corrosion compound to another, the chemical characteristics of iron corrosion scales at different iron release stages are considered. Therefore, the experimental findings of the study will improve our understanding on speciation of iron and development of iron corrosion scales in DWDSs.

2. Materials and methods

2.1. Reagents and solutions

Both deionized water (18.2 MΩ cm, Milli-Q PLUS, Millipore) and tap water were used in the experiments. All solutions were prepared using deionized water. The tap water was collected after the filtration process of South-to-North Water Diversion Project drinking water treatment pilot plants in Danjiangkou (China), whose water quality parameters were summarized in Table 1.

The glassware in the experiments was washed carefully with nitric acid (1:1, v:v) and deionized water. Unless otherwise specified, the chemicals used in the ferrous iron oxidation experiments were of analytical reagent grade and purchased from Tianjin Kemiou Chemical Reagent Co., Ltd, Tianjin, China, which were: $FeSO_4$,·$7H_2O$, NaOH, HCl, Na_2SO_4, NaCl, $NaHCO_3$, NaClO, and NH_4Cl. Monochloramine were prepared with NaClO and NH_4Cl, and then pH was adjusted to 9 with 0.1 mol/L NaOH and 0.1 mol/L HCl, respectively.

Table 1
Quality of filtered water

Parameter	Concentration value
COD_{Mn} (mg/L)	0.89~1.05
TOC (mg/L)	1.70~1.77
pH	8.08~8.14
DO (mg/L)	11.32~11.96
Alkalinity (mg/L as $CaCO_3$)	103.6~127.0
Hardness (mg/L as $CaCO_3$)	132.1~149.0
Sulfate (mg/L)	32.4~34.5
Chloride (mg/L)	7.9~9.0
Fluoride (mg/L)	0.23~0.25
Nitrate (mg/L)	1.12~1.41
TDS (mg/L)	164.2~165.4
Total iron (mg/L)	0~0.03
Langelier index	−0.10~0.25
Larson ratio	0.36~0.45

2.2. Ferrous iron oxidation experiments

The ferrous iron oxidation tests were performed using batch method. These experiments were conducted in six 500 mL sealed iodine flasks by magnetic stirring apparatus. In the beginning, water quality parameters were controlled and measured. An oxygen and nitrogen gas mixture was bubbled through the experimental solution until the DO concentration stabilized. An appropriate amount of chemicals including ferrous iron were then added to the bubbled solution and the concentration of initial ferrous iron was 0.50 ± 0.1 mg/L. The prepared solution was added into the flasks and agitated using magnetic stirrers. After 5, 10, 15, 30, 45, and 60 min of agitating, a solution was orderly taken to determine the residual ferrous iron concentration immediately. At 30 min and 60 min, suspended iron particles were also filtered from the solutions onto 0.45 μm ultrafiltration membrane using a vacuum filtration apparatus. The filtered samples were taken to determine the total iron concentration and the solid materials retained on the ultrafiltration membrane were analyzed in crystalline phase, respectively. In the experiments, the initial total iron concentration equaled initial ferrous iron concentration and the concentration of suspended iron particles that were filtered on 0.45 μm ultrafiltration membrane equaled initial total iron concentration minus total iron concentration in the solutions filtered by 0.45 μm ultrafiltration membrane that is usually defined as the soluble iron concentration.

Table 2
Analysis methods for water quality

Parameter	Examination methods
COD_{Mn}	Acidic potassium permanganate titration method
TOC (mg/L)	Aurora 1030 W TOC analyzer
Turbidity	Hach 2100P turbidimeter
pH/DO/TDS	Hach HQ40d analyzer
Alkalinity	Acid-base indicator titration method
Hardness	EDTA titration method
Sulfate/chloride/fluoride/nitrate	Ion chromatography method
Monochloramine/total chlorine	DPD spectrophotometric method
Ferrous iron/total iron	Naphthisodiazine spectrophotometric method

2.3. Iron corrosion scale development experiments

Cast iron pipes were obtained from the DWDSs of the Tianjin Waterworks Group Co., Ltd, China and constructed as pilot-scale pipe loops for this study. After the corrosion scales and water quality in the pipe loops were stable for a week, corrosion scales were destroyed by changing water quality.

At different iron release stages, typical corrosion scale samples were collected from freshly obtained pipe sections and water samples from the pipe loops were analyzed for the total iron concentration. The pretreatment procedures of scale samples were taken as soon as possible. The samples were pulverized under an anaerobic condition, filtered through a 150 mm mesh sieve, and then dried under a vacuum-freeze condition.

2.4. Chemical analysis

Several sub-samples of pretreated corrosion scales were analyzed to determine the concentrations of total iron, free and amorphous iron which means any iron compounds transported by water flow easily [15]. Duplicate dried samples were digested using HCl, HNO_3, and HF (5.25:1.75:1, v:v:v) and then the total iron concentrations were determined. The free and amorphous irons were extracted by dithionite-citrate-bicarbonate technique in accordance with the method described by Tan [15,18]. Iron compounds in crystalline phase were identified by X-ray diffraction (XRD) (RIGAKU D/MAX 2500V/PC, Japan).

The analysis methods of water quality including permanganate index (COD_{Mn}), total organic carbon (TOC), turbidity, pH, DO, total dissolved solids (TDS), alkalinity, hardness, sulfate, chloride, fluoride, nitrate, monochloramine, total chlorine, ferrous iron, and total iron are shown in Table 2.

3. Results and discussion

3.1. Effect of water quality on ferrous iron oxidation

Iron is released from distribution system materials only as ferrous form through chemical reactions [6] and oxidation of ferrous iron to relatively insoluble ferric iron is an important reaction in DWDSs. As can be seen in Fig. 1, oxygen was a weak oxidant and its oxidation rate was strongly dependent on pH. Under conditions of constant pH and temperature, the difference of ferrous iron oxygenation rate was not significant as DO concentration increased from 2.49 to 8.46 mg/L with an initial ferrous iron concentration of 0.57 mg/L because the oxygen concentration was sufficient for the ferrous iron oxidation reaction. The ferrous iron oxygenation rate increased as pH increased, and the rate was also influenced by alkalinity. The oxygenation rate significantly increased with increasing pH over the range of 7.03–7.89. At the time of 30 min, the ferrous iron concentration decreased from the initial concentration of 0.57–0 mg/L at pH 7.89 while that concentration decreased from 0.57 to 0.50 mg/L at pH 7.03. Fig. 1(c) revealed the ferrous iron oxygenation rate increased with increasing alkalinity, which was attributed to the formation of $FeCO_3$ with increasing HCO_3^- whose concentration is equal to the alkalinity when pH is 6.0~8.5 and the oxidation rate of $FeCO_3$ which is thought to be faster than that of $Fe(OH)_2$ [19]. Fig. 1(d) and (e) showed that increase of sulfate and chloride had a slight effect on the ferrous iron oxygenation rate, respectively.

Monochloramine is another main oxidant in the DWDSs. When strong oxidants such as free chlorine and monochloramine are present in drinking water at significant concentrations, they can react rapidly with oxidizable materials (e.g. micro-organisms, organic matter, and reduced iron phases). Fig. 1(f) illustrated

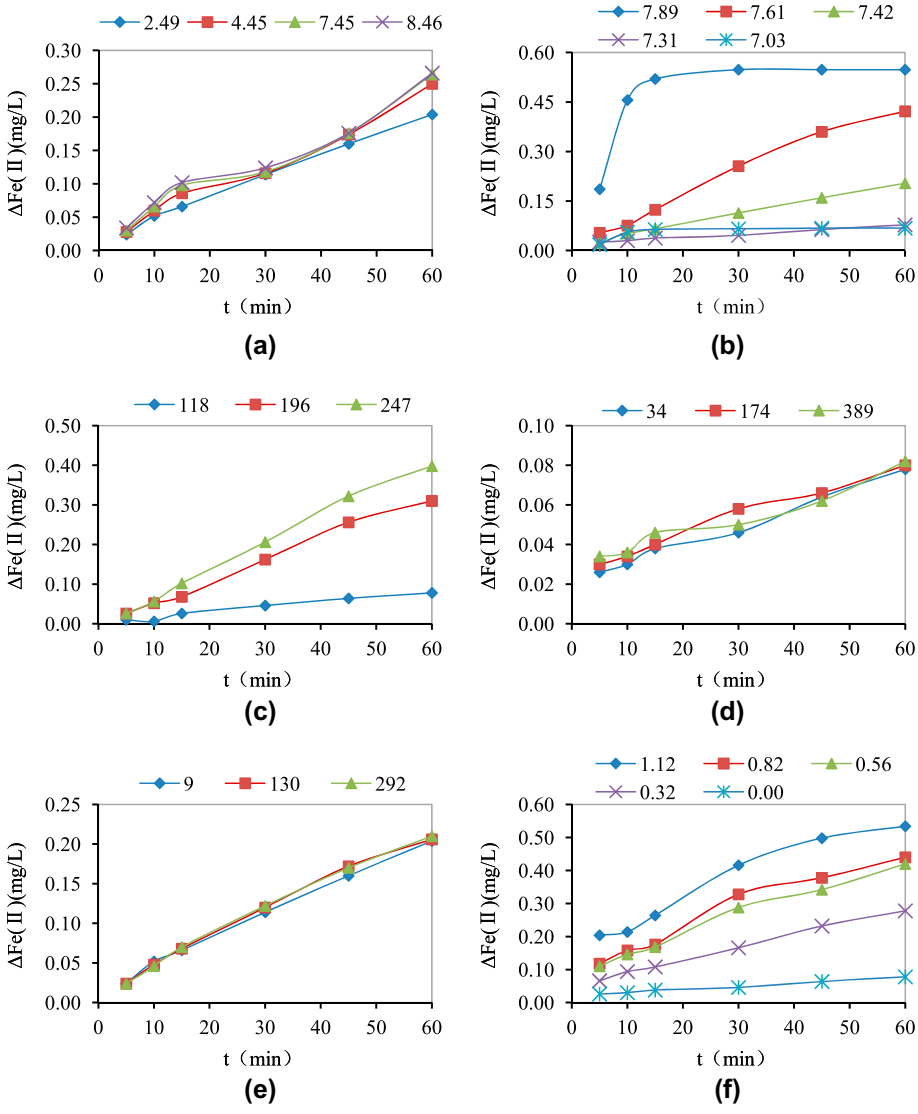

Fig. 1. Effect of water quality on ferrous iron oxidation (a) DO; (b) pH; (c) alkalinity; (d) sulfate; (e) chloride; (f) monochloramine.

that the ferrous iron oxidation rate rose with increasing monochloramine concentration (as Cl_2) from 0 to 1.12 mg/L.

3.2. Oxidation kinetics

The oxidation kinetics of ferrous iron to ferric iron are important in many environmental application, including bioavailability of iron to aquatic organisms, acid mine drainage, and DWDS issues. In order to describe the oxidation kinetics, the kinetics equation is commonly used. The kinetics of ferrous iron oxygenation in laboratory systems have been previously studied [20–22] and the general rate law was reported as:

$$-\frac{dC_{Fe^{2+}}}{dt} = kC_{Fe^{2+}}P_{O_2}C_{OH^-}^2 \quad (1)$$

where k is oxidation reaction rate constant with unit of $(mol/L)^{-2}\,atm^{-1}\,min^{-1}$, and $C_{Fe^{2+}}$, P_{O_2} and C_{OH}^- denote total ferrous iron concentration (mg/L), partial pressure of oxygen in gas phase in equilibrium with the water (atm), and hydroxyl ion concentration (mol/L), respectively.

Holding pH and O_2 constant, Equation 1 integrates to:

$$C_{Fe^{2+}} = C_{Fe^{2+}}^0 e^{-k_1 t} \quad (2)$$

where $k_1 = kP_{O_2}C^2_{OH^-}$ (min^{-1}) and $C^0_{Fe^{2+}}$ is the initial ferrous iron concentration (mg/L).

A summary of the corresponding experimental conditions, k_1 and the correlation coefficient (R^2) fitted by origin software for the kinetics model is shown in Table 3. From Table 3, it can be seen that the R^2 of the monochloramine oxidation kinetics model are 0.951~0.964, which means that Equation 2 is also applicable to the ferrous iron oxidation reaction when monochloramine exists in the drinking water. When pH is low (e.g. pH 7.03), the oxygenation reaction rate is small and the oxidation kinetics model in a short span of time cannot describe the oxygenation reaction process properly.

3.3. Effect of water quality on iron suspensions

"Colored water" resulting from suspended iron particles (>0.45 μm), which is largely impacted by water quality, is a common drinking water consumer complaint. The actual suspension color may range from light yellow to red due to the forms of iron which can originate from source water and/or from pipe materials. The relatively soluble ferrous iron is the dominant form of iron found in anoxic environments (e.g. DWDS dead ends and the area beneath thick iron corrosion scales). When exposed to oxygen or disinfection, ferrous iron is oxidized to the insoluble ferric iron, which can produce a certain level of chromaticity and turbidity. Fig. 2 illustrates the concentrations of iron as suspended particles are positively correlated with the increasing turbidity values in actual DWDSs.

The effect of water quality on suspended iron particle mass fraction (iron concentration filtered on 0.45 μm ultrafiltration membrane/initial iron concentration, %) is presented in Fig. 3. With pH being controlled at 7.45 (±0.05) and the initial DO concentration ranging between 2.49 and 8.46 mg/L, which reflected seasonal variation of concentration in the drinking water, the suspended iron particle mass fraction increased slightly. When the initial DO concentration was controlled at 2.46 (±0.45), the suspended iron particle mass fraction increased dramatically with increasing pH from 7.03 to 7.89. With increasing alkalinity over the range of 118 to 247 mg/L, the suspended iron particle mass fraction increased significantly when the initial DO concentration and pH were controlled at 2.46 (±0.45) and 7.31, respectively. The changes of sulfate and chloride had little or no effect on the suspended iron particle mass fraction. The suspended iron particle mass fraction increased with the monochloramine concentration rising. What's more, when the reaction time was prolonged, the suspended iron particle mass fraction increased.

XRD analysis of iron suspensions on the surface of ultrafiltration membrane indicated the presence of siderite ($FeCO_3$), goethite (α-FeOOH), akaganeite (β-FeOOH), magnetite (Fe_3O_4), lepidocrocite (γ-FeOOH), hematite (Fe_2O_3), and green rust, which are in accordance with the crystalline phase of iron corrosion scales.

Table 3
Kinetic parameters under corresponding experimental conditions

DO (mg/L)	pH	Alkalinity (mg/L)	Sulfate (mg/L)	Chloride (mg/L)	Monochloramine (mg/L)	k_1 (min^{-1})	R^2
2.49	7.42	118	34	9	–	0.0084	0.996
4.45	7.42	118	34	9	–	0.0093	0.976
7.45	7.42	118	34	9	–	0.0096	0.959
8.46	7.42	118	34	9	–	0.0098	0.953
2.49	7.03	118	34	9	–	0.0028	0.112
2.49	7.31	118	34	9	–	0.0023	0.782
2.49	7.61	118	34	9	–	0.0239	0.979
2.49	7.89	118	34	9	–	0.1303	0.954
2.49	7.31	196	34	9	–	0.0141	0.977
2.49	7.31	247	34	9	–	0.0163	0.973
2.49	7.31	118	174	9	–	0.0033	0.910
2.49	7.31	118	289	9	–	0.0034	0.925
2.49	7.42	118	34	130	–	0.0075	0.996
2.49	7.42	118	34	292	–	0.0076	0.998
2.49	7.31	118	34	9	0.32	0.0100	0.951
2.49	7.31	118	34	9	0.56	0.0190	0.961
2.49	7.31	118	34	9	0.82	0.0220	0.964
2.49	7.31	118	34	9	1.12	0.0472	0.963

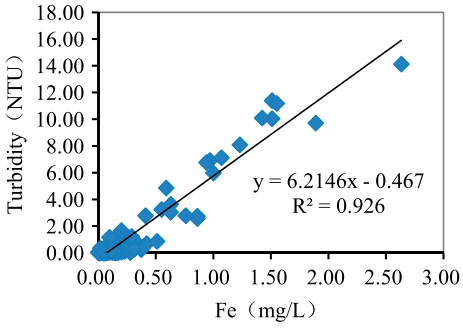

Fig. 2. Relationship between concentrations of suspended iron particles and increasing turbidity values.

3.4. Development of iron corrosion scales

Based on the XRD analysis of iron suspensions on the surface of ultrafiltration membrane, iron compounds in crystalline phase of different iron released stages were identified and the results of two representative samples are shown in Table 4. Because the experimental iron pipes were old and had heavily corroded inner surfaces, the iron corrosion scales mainly consisted of two distinct regions: hard shell-like layer (HSL) and porous core layer (PCL). Old unlined cast iron pipe sample A and B that were of 100 mm diameter and had been used for more than 20 years were excavated from two different sites of DWDSs, which were supplied with finished water from the Luanhe

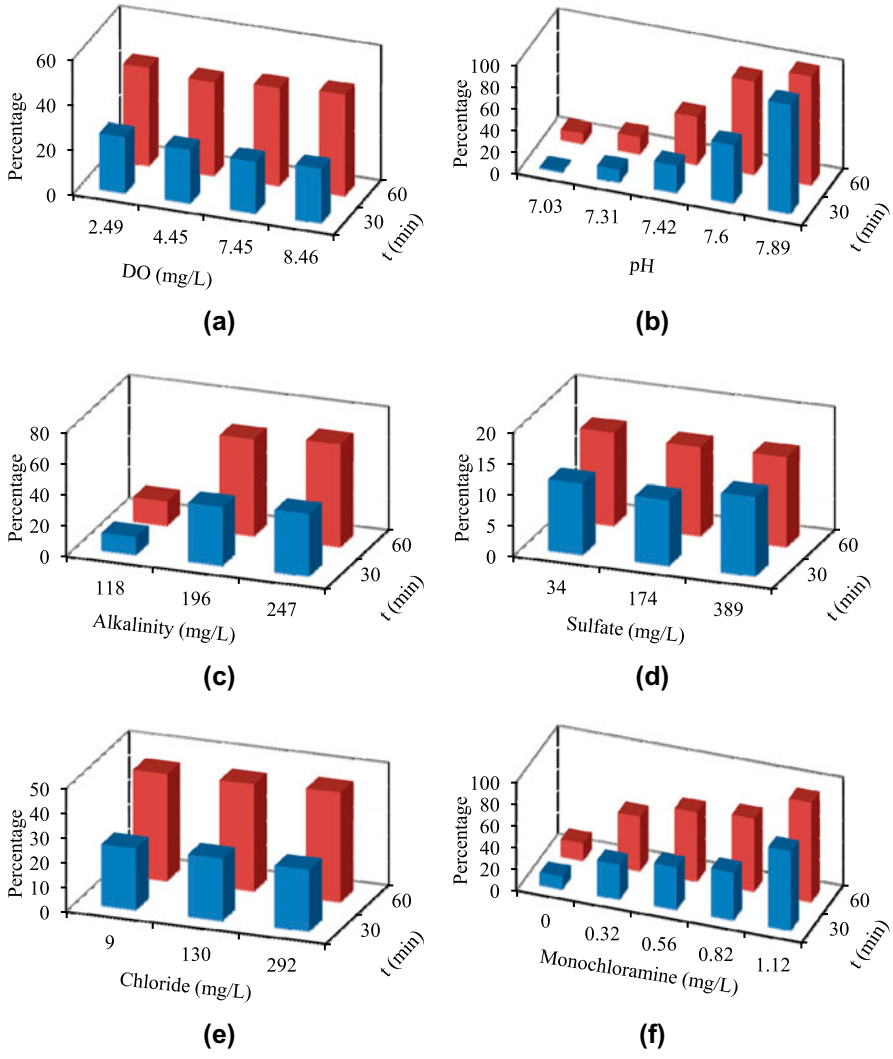

Fig. 3. Effect of water quality on suspended iron particle mass fraction (a) DO; (b) pH; (c) alkalinity; (d) sulfate; (e) chloride; (f) monochloramine.

Table 4
Change of iron compounds in corrosion scales

Sample	Compound	Initial stage		60th day		150th day	
		HSL	PCL	HSL	PCL	HSL	PCL
A	Magnetite (%)	10	6	46	55	56	75
	Goethite (%)	12	3	26	14	33	25
	Lepidocrocite (%)	4	2	6	5	11	–
	Siderite (%)	–	4	–	9	–	–
	Green rust (%)	74	85	22	17	–	–
B	Magnetite (%)	3	–	24	15	28	30
	Goethite (%)	2	–	25	15	50	46
	Akaganeite (%)	6	9	–	14	–	–
	Lepidocrocite (%)	2	3	6	7	8	5
	Green rust (%)	87	88	45	49	14	19

Table 5
Quality of feed water at different stages

	Stage 1 Initial stage	Stage 2 Initial stage~60th day	Stage 3 60th day~150th day
DO (mg/L)	0.5~5.5	8.10~9.52	9.91~11.50
pH	7.78~7.92	7.91~8.09	8.16~8.31
Alkalinity (mg/L)	89.0~93.7	93.2~103.5	99.1~119.8
Hardness (mg/L)	107.3~117.3	112.5~123.9	120.4~138.2
Sulfate (mg/L)	22.8~24.3	24.8~25.3	26~27.2
Chloride (mg/L)	3.26~5.31	3.57~5.62	3.78~6.02
Total chlorine (mg/L)	0.08~0.61	0.20~0.80	0.19~0.82

River. In the initial experiment stage, the iron corrosion scales in pipe inner surfaces had been destroyed by water quality that is shown in Table 5 and the iron was released seriously with the maximum value of iron concentration being above 1.0 mg/L. With the development of time and water quality back to normal, the iron release level dropped and the average iron concentration from the 20th day to the 60th day was 0.15 mg/L. In the third stage, the average iron concentration was 0.08 mg/L.

It is observed from Table 5 that the water quality of initial stage was characterized by low DO, pH, and alkalinity, which could occur in poorly managed DWDSs. From Table 4, it can be seen that in the initial stage, green rust was the main component of iron corrosion scales, which is instable and an intermediate compound between the initial iron corrosion product and the iron oxyhydroxides [23–26]. With the water quality and iron release amount being relatively stable, green rust mass reduced and the mass of both magnetite and goethite of good chemical stability increased, which finally dominated the iron corrosion scales.

The mass fractions of both the total iron in iron corrosion scales and the free and amorphous iron in the total iron which changed in different iron release stages are illustrated in Figs. 4 and 5. When the iron release level was high, the newly formed free and amorphous iron contents (e.g. $Fe(OH)_2$ and $Fe(OH)_3$) increased. What's more, one part of the iron released from pipe materials entered the waters and the other

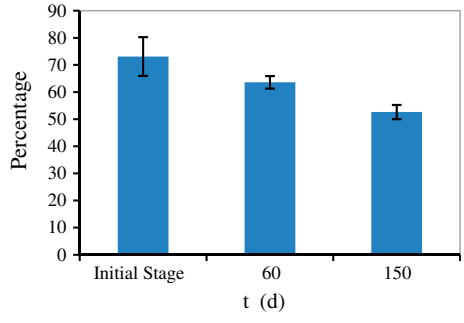

Fig. 4. Mass fraction change of the total iron in iron corrosion scales.

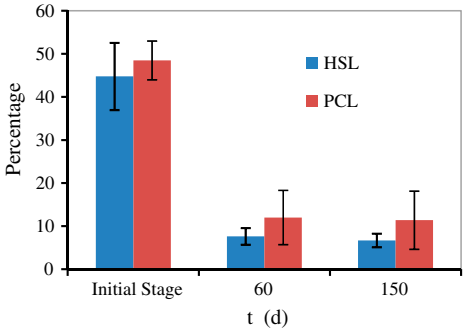

Fig. 5. Mass fraction change of the free and amorphous iron in the total iron.

part precipitated on the corroded inner surfaces of pipes, which resulted in the mass fraction of the total iron in iron corrosion scales rising. With the iron release amount reducing and the free and amorphous iron having coming into the water distribution system already, both the free and amorphous iron contents and the total iron in iron corrosion scales decreased.

4. Conclusions

With iron being released from distribution system materials only as ferrous form through chemical reactions, water quality had impacts on iron oxidation rate and suspended iron particles whose concentrations are positively correlated with the increasing turbidity value. Alkalinity, pH, and monochloramine had significant impacts on iron oxidation rate and suspended iron particle, and DO, sulfate, and chloride had a slight effect on iron oxidation rate and suspended iron particle. What's more, when the reaction time was prolonged, the mass fraction of suspended iron particles increased. Except at low pH (e.g. pH 7.03), the oxygenation process of ferrous iron to ferric iron can be well described by oxidation kinetics model which also fits the oxidation reaction of ferrous iron to ferric iron by monochloramine.

With water quality having destroyed pipe corrosion scales, the iron release level rose which impacted the chemical composition of corrosion scales and the iron mass fractions in corrosion scales. In the initial experiment stage when the iron was released seriously, the newly formed free and amorphous iron contents (e.g. $Fe(OH)_2$ and $Fe(OH)_3$) increased, instable iron compounds dominated the iron corrosion scales and the mass fraction of the total iron in iron corrosion scales rose. With the iron release amount being relatively stable, the free and amorphous iron contents dropped, magnetite and goethite were the main components of iron corrosion scales, and the total iron in iron corrosion scales decreased.

Acknowledgments

This work was funded by Tianjin Science and Technology Project (11ZCKFSF01700) and Water Pollution Controls and Treatment Technologies Special Project of China (2012X07404002).

References

[1] J.H.G. Vreeburg, J.B. Boxall, Discolouration in potable water distribution systems: A review, Water Res. 41 (2007) 519–529.
[2] M. Edwards, Controlling corrosion in drinking water distribution systems: A grand challenge for the 21st century, Water Sci. Technol. 49 (2004) 1–8.
[3] Z.B. Niu, Y. Wang, X.J. Zhang, W.J. He, H.D. Han, P.J. Yin, Iron stability in drinking water distribution systems in a city of China, J. Environ. Sci. 18 (2006) 40–46.
[4] H.Z. Liu, K.D. Schonberger, C.Y. Peng, J.F. Ferguson, E. Desormeaux, P. Meyerhofer, H. Luckenbach, G.V. Korshin, Effects of blending of desalinated and conventionally treated surface water on iron corrosion and its release from corroding surfaces and pre-existing scales, Water Res. 47 (2013) 3817–3826.
[5] M.R. Lasheen, C.M. Sharaby, N.G. El-Kholy, I.Y. Elsherif, S.T. El-Wakeel, Factors influencing lead and iron release from some Egyptian drinking water pipes, J. Hazard. Mater. 160 (2008) 675–680.
[6] P. Sarin, V.L. Snoeyink, D.A. Lytle, W.M. Kriven, Iron corrosion scales: Model for scale growth, iron release, and colored water formation, J. Environ. Eng. 130 (2004) 364–373.
[7] S.A. Imran, J.D. Dietz, G. Mutoti, J.S. Taylor, A.A. Randall, Modified Larsons Ratio incorporating temperature, water age, and electroneutrality effects on red water release, J. Environ. Eng. 131 (2005) 1514–1520.
[8] Z.J. Tang, S.K. Hong, W.Z. Xiao, J. Taylor, Characteristics of iron corrosion scales established under blending of ground, surface, and saline waters and their impacts on iron release in the pipe distribution system, Corros. Sci. 48 (2006) 322–342.
[9] P. Sarin, V.L. Snoeyink, J. Bebee, K.K. Jim, M.A. Beckett, W.M. Kriven, J.A. Clement, Iron release from corroded iron pipes in drinking water distribution systems: Effect of dissolved oxygen, Water Res. 38 (2004) 1259–1269.
[10] J.Y. Lee, C.R. Pearson, R.M. Hozalski, W.A. Arnold, Degradation of trichloronitromethane by iron water main corrosion products, Water Res. 42 (2008) 2043–2050.
[11] S.C. Morton, Y. Zhang, M.A. Edwards, Implications of nutrient release from iron metal for microbial regrowth in water distribution systems, Water Res. 39 (2005) 2883–2892.
[12] L.A. Rossman, The effect of advanced treatment on chlorine decay in metallic pipes, Water Res. 40 (2006) 2493–2502.
[13] Z. Zhang, J.E. Stout, V.L. Yu, R. Vidic, Effect of pipe corrosion scales on chlorine dioxide consumption in drinking water distribution systems, Water Res. 42 (2008) 129–136.
[14] T.L. Gerke, J.B. Maynard, M.R. Schock, D.L. Lytle, Physiochemical characterization of five iron tubercles

from a single drinking water distribution system: Possible new insights on their formation and growth, Corros. Sci. 50 (2008) 2030–2039.
[15] J.P. Lin, M. Ellaway, R. Adrien, Study of corrosion material accumulated on the inner wall of steel water pipe, Corros. Sci. 43 (2001) 2065–2081.
[16] R.I. Ray, J.S. Lee, B.J. Little, T.L. Gerke, The anatomy of tubercles: A corrosion study in a fresh water estuary, Mater. Corros. 61 (2010) 993–999.
[17] F. Yang, B.Y. Shi, J.N. Gu, D.S. Wang, M. Yang, Morphological and physicochemical characteristics of iron corrosion scales formed under different water source histories in a drinking water distribution system, Water Res. 46 (2012) 5423–5433.
[18] K.H. Tan, Soil Sampling, Preparation, and Analysis, Marcel Dekker, New York, NY, 1996.
[19] F.J. Millero, The effect of ionic interactions on the oxidation of metals in natural waters, Geochim. Cosmochim. Acta 49 (1985) 547–553.
[20] F.J. Millero, S. Sotolongo, M. Izaguirre, The oxidation kinetics of Fe(II) in seawater, Geochim. Cosmochim. Acta 51 (1987) 793–801.
[21] W. Davison, G. Seed, The kinetics of the oxidation of ferrous iron in synthetic and natural waters, Geochim. Cosmochim. Acta 47 (1983) 67–79.
[22] E.J. Roekens, R. Van Grieken, Kinetics of iron(II) oxidation in seawater of various pH, Mar. Chem. 13 (1983) 195–202.
[23] H. Drissi, P. Refait, J.M.R. Génin, The oxidation of Fe $(OH)_2$ in the presence of carbonate ions: Structure of carbonate green rust one, Hyperfine Interact. 90 (1994) 395–400.
[24] P. Refait, M. Abdelmoula, J.M.R. GÉnin, Mechanisms of formation and structure of green rust one in aqueous corrosion of iron in the presence of chloride ions, Corros. Sci. 40 (1998) 1547–1560.
[25] A.A. Olowe, J.M.R. Genin, P. Bauer, Hyperfine interactions and structures of ferrous hydroxide and green rust II in sulfated aqueous media, Hyperfine Interact. 41 (1988) 501–504.
[26] J. Świetlik, U. Raczyk-Stanisławiak, P. Piszora, J. Nawrocki, Corrosion in drinking water pipes: The importance of green rusts, Water Res. 46 (2012) 1–10.